Health Research Alliance
Member Organization Author Manuscript
Arch Biochem Biophys. Author manuscript; available in PMC 2021 December 01.

Published in final edited form as:
Arch Biochem Biophys. 2021 August 15; 707: 108909. doi:10.1016/j.abb.2021.108909.

Reduced preload increases Mechanical Control (strain-rate dependence) of Relaxation by modifying myosin kinetics

Brianna M. Schick[1], **Hunter Dlugas**[1], **Teresa L. Czeiszperger**, **Alexandra R. Matus**, **Melissa J. Bukowski**, **Charles S. Chung**[*]
Department of Physiology, Wayne State University, Detroit, MI, USA

Abstract

Rapid myocardial relaxation is essential in maintaining cardiac output, and impaired relaxation is an early indicator of diastolic dysfunction. While the biochemical modifiers of relaxation are well known to include calcium handling, thin filament activation, and myosin kinetics, biophysical and biomechanical modifiers can also alter relaxation. We have previously shown that the relaxation rate is increased by an increasing strain rate, not a reduction in afterload. The slope of the relaxation rate to strain rate relationship defines Mechanical Control of Relaxation (MCR). To investigate MCR further, we performed in vitro experiments and computational modeling of preload-adjustment using intact rat cardiac trabeculae. Trabeculae studies are often performed using isometric (fixed-end) muscles at optimal length (Lo, length producing maximal developed force). We determined that reducing muscle length from Lo increased MCR by 20%, meaning that reducing preload could substantially increase the sensitivity of the relaxation rate to the strain rate. We subsequently used computational modeling to predict mechanisms that might underlie this preload-dependence. Computational modeling was not able to fully replicate experimental data, but suggested that thin-filament properties are not sufficient to explain preload-dependence of MCR because the model required the thin-filament to become more activated at reduced preloads. The models suggested that myosin kinetics may underlie the increase in MCR at reduced preload, an effect that can be enhanced by force-dependence. Relaxation can be modified and enhanced by reduced preload. Computational modeling implicates myosin-based targets for treatment of diastolic dysfunction, but further model refinements are needed to fully replicate experimental data.

Keywords

Trabeculae; Relaxation; Myofiber; Modeling; Biomechanics

This is an open access article under the CC BY-NC-ND license (http://creativecommons.org/licenses/by-nc-nd/4.0/).

[*]Corresponding author. Department of Physiology Wayne State University, Rm 5374 Scott Hall 540 E Canfield, Detroit, MI, 48201, USA. cchung@med.wayne.edu (C.S. Chung).
[1]Equal Contribution.

Declaration of competing interest
None.

Appendix A. Supplementary data
Supplementary data to this article can be found online at https://doi.org/10.1016/j.abb.2021.108909.

Health Research Alliance Author Manuscript
Health Research Alliance Author Manuscript

Health Research Alliance Author Manuscript

Health Research Alliance Author Manuscript

1. Introduction

Impaired cardiac relaxation is considered the first sign of diastolic dysfunction and is an important diagnostic feature of heart failure with preserved ejection fraction (HFpEF) [1,2]. Biochemically, relaxation is well known to be controlled by calcium removal from the cytosol, thin filament deactivation, and myosin-actin crossbridge detachment kinetics [3]. Because these processes are simply a reversal of the biochemical processes that drive contraction, the same processes likely underlie a well-known contraction-relaxation coupling that is dependent primarily on sarcomeric properties [4]. This coupling has been recently observed in human myocardium in vitro [5]. One limitation of most in vitro myocardial studies is that they typically assess relaxation during fixed-end (muscle length isometric) twitches. In contrast, length changes occur during physiologic contraction and relaxation in response to the arterial afterload. Indeed, recent results suggest that contraction and relaxation can become uncoupled in an in vivo canine model [6].

Afterload, or the pressure against which the heart ejects, has been thought to be a modifier of myocardial relaxation [7]. However, it was previously shown that a lengthening myocardial strain (sometimes referred to as ‘relaxation loading’) is necessary for afterload-dependence to be revealed [8,9]. We have recently shown that the lengthening strain is sufficient to mechanically modify relaxation, independent of the afterload, and that the relaxation rate is dependent on the strain rate [10]. The slope of the relationship between the relaxation rate and the strain rate indicates how sensitive the muscle’s relaxation rate is to stretch, and we define this slope as Mechanical Control of Relaxation (MCR). Increasing MCR, i.e. increasing this slope, may improve myocardial relaxation without any changes in the isoforms of proteins that are typically thought to underlie relaxation. Our prior study focused on muscles set to the length where optimal developed force was obtained (Lo). However, cardiac muscles typically function at shorter sarcomere lengths in vivo [11,12]. The muscle length prior to contraction, which we refer to as preload in this study, is also modified by therapeutics such as diuretics which reduce ventricular volume. In the current study, we utilized preload reduction in intact cardiac trabeculae and computational modeling to reveal mechanisms underlying the MCR.

This study reveals that Mechanical Control of Relaxation is preload-dependent. Computational modeling was used to predict the responsible mechanisms by testing parameters previously shown to be preload-dependent, such as thin filament overlap, titin stiffness, myosin ADP release rate, and troponin calcium sensitivity [13-19]. Physiologic changes to the thin filament (i.e. reduced activation at reduced preload) was not consistent with an increased MCR. We further evaluated additional model variables, including strain-rate-dependent myosin detachment to identify potential molecular mechanisms underlying Mechanical Control of Relaxation. These data have potential biophysical and clinical application.

Health Research Alliance Author Manuscript

Health Research Alliance Author Manuscript

2. Methods

2.1. Intact trabeculae mechanical experiments

Animal use was approved by the Institutional Animal Use and Care Committee of Wayne State University.

Data reported are derived from 14 intact cardiac muscle strips (trabeculae) isolated from individual female Sprague Dawley rats (4.3 ± 1.1 months) as previously described [10]. Two strips were from the left ventricle and 12 from the right ventricle; two were right ventricular papillary muscles. Briefly, each rat was anesthetized under isoflurane anesthesia and euthanized by exsanguination. The heart was quickly rinsed with 4 °C oxygenated perfusion solution (in mM: 113 NaCl, 4.7 KCl, 0.6 KH2PO4, 1.2 MgSO4, 12 NaHCO3, 10 KHCO3, 10 2-[4-2-hydroxyethyl)piperazin-1-yl]ethanesulfonic acid (HEPES), 30 Taurine, 5.5 glucose, 10 2,3-butanedione monoxine (BDM)), cannulated, and briefly Langendorff perfused to remove excess blood. Free-standing cardiac trabeculae (or papillary muscles), including myocardial segments that allowed the trabeculae to be mounted without damage, were used. The myocardial segments of each trabecula were mounted on hooks between a length motor and a force transducer in an experimental chamber (801C-1900, Aurora Scientific, Aurora ON Canada) and continuously super-fused with oxygenated Tyrode's solution (in mM: 140 NaCl, 5.4 KCl, 1.8 CaCl2, 1 MgCl2, 10 HEPES, 10 glucose) at 25 °C. The muscle was paced at 0.5Hz (Myopacer, IonOptix West-wood, MA) and stretched to optimal length (Lo) where maximal developed force was achieved during muscle length isometric (fixed-end) contraction. The pin-to-pin distance, the trabecula length (Fig. 1C), and diameter were then measured; the cross-sectional area (CSA) was calculated from the average of 4 diameters measurements assuming a cylindrical cross-section. The muscle was allowed to equilibrate for 1 h prior to experiment.

SLControl software was used to perform feedback-controlled afterload clamps on the cardiac trabeculae and acquire force, length, and pacing/gating information [10,20]. The ends of each trabecula were held fixed except when afterload clamps were being performed. Afterload clamps were performed at least 6 s apart to prevent history-dependent effects. During the afterload clamp trials, the trabeculae were load clamped by shortening the muscle at a predetermined force (mimicking afterload). To study the relationship between strain rate and relaxation rate, the length motor relengthened the trabecula at varying speeds (strain rates) at a specific afterload before they were allowed to relax with the muscle ends held fixed. Subsequently, the motor relengthened the muscle back to the resting length, if necessary. Afterload clamps were performed at 25% and 50% of the maximum developed force. After performing feedback-controlled afterload clamps at Lo as described, the muscle length (preload) was adjusted to study the effect of preload on the relationship between strain rate and relaxation rate. A micromanipulator was used to shorten the muscle length by 5% of the pin-to-pin distance, resulting in a trabecula shortening of 5–12%. The muscle was then allowed to equilibrate for 20 min at the reduced preload before data acquisition in order to avoid slow force response effects [16,21,22]. Feedback-controlled afterload clamps were then performed following the same protocol that was used at Lo. An example of fixed-end and load-clamped data for Lo and reduced preload are shown in Fig. 1. Once data

Health Research Alliance Author Manuscript

Health Research Alliance Author Manuscript

acquisition was completed at the lowered preload, the muscle was manually relengthened back to Lo. Experiments were terminated if the maximum developed force decreased by >20%. Muscles were excluded from analysis if they became arrhythmic during the protocol or had a developed force below 10 mN/mm^2 at Lo.

Data were analyzed offline using custom scripts written in MATLAB (Mathworks, Natick MA) and in Microsoft Excel (Microsoft Corporation, Redmond WA) as previously described [10]. Briefly, tension was calculated by dividing the force by the CSA at Lo and both tension and length signals were smoothed using a Savitzky-Golay filter before calculating the derivative of each signal with respect to time. Strain rate was calculated from the time derivative of length divided by the length of the trabecula at Lo. Relaxation rate of tension was calculated using the Glantz method [10,23] starting at the minimum time derivative of tension. Peak contractile and minimum (end diastolic) tension were calculated for each load clamp and for fixed-end beats at each condition; developed tension was calculated as the difference between the peak and minimum tension. The lengthening strain rate preceding the relaxation was determined for each load clamp.

Mechanical Control of Relaxation, i.e. the slope of the relationship between the relaxation rate and peak lengthening strain rate, was determined (example shown in Supplemental Figure 1). To minimize variance in the independent axis (strain rate), data was limited to a strain rate of ~1.0 s^{-1}, which was achieved by all but one of the samples and is within a physiologic strain rate. The minimum strain rate was limited to ~0.12 s^{-1} due to non-linear changes in the minimum time derivative of tension. Linear regression was performed to determine the slopes. The absolute and percent changes in slope were calculated.

2.2. Computational modeling

Twitch contractions were simulated using a mathematical model consisting of a single half sarcomere connected in series to an elastic spring using MyoSim (version 2.5) [18,24]. Experimental data (tension, calcium) were obtained from a single trabecula as previously described [10,24]. The calcium transient was determined from a Fura-2AM loaded trabecula. Briefly, pacing and Tyrode's superfusion in the experimental chamber (1.8 mL volume) was stopped, and the regular Tyrode's solution replaced with Fura-2AM supplemented Tyrode's Solution (2 μM Fura-2AM, 0.17% pluronic acid, 17 μL/mL DMSO, 8.3 μL/mL Kolliphor EL) using three exchanges of 50% of the chamber volume and incubated at 25 °C for 2 h. The chamber was then washed out with 30–50 mL of normal Tyrode's solution and pacing resumed; the muscle was allowed to equilibrate again for approximately 45 min. Calcium transients were measured as previously described using a photometer to measure the Fura-2 fluorescence at 510 nm in response to dual wavelength excitation at 340 and 380 nm at 250 Hz. The shape of the calcium transient was determined using a bi-exponential function [10,25]. Calcium concentrations were taken from previous reports and the diastolic calcium was fixed at pCa 6.7, while peak calcium was fixed at pCa 6.10 and 6.26 for Lo and reduced preload, respectively [26-28].

Model fits were performed as previously defined [18,24]. Briefly, the above calcium transient was defined in each model, and the initial half sarcomere length was defined as 1.15 μm. A 200 ms period was used to ensure the model reached a steady-state passive

Health Research Alliance Author Manuscript

Health Research Alliance Author Manuscript

condition prior to initiation of the calcium transient. Modeling began with a two-state myosin kinetic system with an attached and detached state. Parameters that defined the transition rates between the parameters were defined in the model (kinetic schemes are shown in Supplemental Figure 2A). The two states represent attached and detached states with transition rates equivalent to the traditional “f” and “g” rates [24,25]. The model was first fit to experimental tension traces of fixed-end twitches at two preloads. The passive stiffness and series elastic parameters were then fixed, and the model was fit separately at each preload to data including both fixed-end and load clamp twitches. All fits were allowed to run for more than 100 iterations, until the normalized fit error reached a plateau with a value typically below 0.06. For each load-clamp condition included, a fixed-end twitch of the same preload was included to ensure that load-clamp conditions were not weighted more than the fixed-end conditions. MCR was then calculated from the strain rate and relaxation rate of the model fit at each preload. To minimize variance in the independent axis (strain rate) and to prevent models from overshooting their resting position, MCR was calculated using strain rates up to approximately 0.15 s^{-1}. Subsequently, a three-state myosin kinetic scheme, with one detached state, an attached state, and a post-power-stroke state (Supplemental Figure 2B) was fit as above. Reverse rates were held to zero because the model fit including such a transition resulted in a sudden drop in forces, followed by a slight force recovery, where experimental data were otherwise decaying (Supplemental Figure 5). The three-state system was also used to evaluate whether non-myosin parameters might control preload-dependence of Mechanical Control of Relaxation by manually scaling the adjustable parameters. Force-dependence was then added to individual myosin parameters, creating new models. (Note that force-dependence here is actually tension dependence, but we use this terminology to be consistent with other model descriptions [18].) First, force-dependence was also added for the transition into a sequestered detached state of a separate three-state system with one attached state and two detached states (Supplemental Figure 2A). The sequestered detached state was previously used to describe the super relaxed state (SRX) [18]. In the previous study, the SRX was shown to be required to provide accurate fit to fixed-end isometric twitches in muscles. Force-dependence was defined individually for each myosin transition rate magnitude and for the strain sensitivity of the detachment rate, scaling the transition rate parameter(s) proportionally to the developed force. Models with multiple force-dependent parameters were also evaluated. Each model was then fit simultaneously to load-clamp data at both preloads and Mechanical Control of Relaxation was calculated as described above.

2.3. Statistical analysis

Linear regression was performed in Microsoft Excel. Statistics were performed using paired and one-sample t-tests in SPSS (Ver 26, IBM Corporation, Armonk, NY).

3. Results

Baseline muscle parameters are included in Table 1. Experimentally, pin-to-pin length was reduced by approximately 5% (4.88 ± 0.11%) while muscle length was reduced by 7.94 ± 2.09%. This reduction in preload reduced developed tension by 56 ± 12% and increased the relaxation rate of fixed-end twitches by 20 ± 23%. Mechanical Control of Relaxation

Health Research Alliance Author Manuscript

Health Research Alliance Author Manuscript

(MCR) was calculated for all 14 muscles at Lo and reduced preload (0.95 relative to the pin-to-pin Lo length) (Table 2). On average, MCR was increased by 20 ± 21% (Fig. 2). Preload-dependence of MCR was repeatable (Supplemental Fig. 3), and the linearity of MCR versus preload was also confirmed (Supplemental Fig. 4). Multiple linear regression showed that MCR was not dependent on CSA or muscle length (data not shown). However, we identified a reduction in slope for 4 out of the 14 samples (Fig. 2). Upon further inspection of the muscles, we identified that the 4 samples were a subset of 6 muscles that had possible irregular attachments. The attachments were associated with unusual compliance that was visualized as either chordae from a papillary muscle, a mis-placed hook near the end of the large muscular region, or holes or tears within the trabeculae. Notably, muscles with such compliant attachments did not differ from the other samples in their length, CSA, or fixed-end isometric tension parameters except for minimum (diastolic) tension (Supplementary Table 1). This finding suggests that the compliant attachment did not substantially modify the function of the muscle during the fixed-end isometric twitches, only during the dynamic load-clamping twitches.

We then used computational modeling to predict sarcomeric mechanisms that were associated with the preload-dependence of MCR utilizing the MyoSim simulation environment [24]. The model was driven by a calcium transient and fit to data taken from one trabecula. No differences were observed in the ratios nor timing of transients (data not shown), so only one fit was performed to determine the time course of the cytosolic calcium concentration, and the peak and minimum calcium concentrations estimated based on published results [26-28]. After defining the calcium transient, multiple models based on two- or three-state myosin kinetic states (Supplemental Figure 2) were fit to the data as described in the methods.

The fits for all of the models did not fully replicate either the fixed-end isometric or load-clamp experimental data (Fig. 3). The models produced length changes and strain rates below that observed in experimental trabeculae. Furthermore, the models resulted in relaxation rates that far exceeded those quantified from experimental data at equivalent strain rates, resulting in much larger MCR values.

Initial fitting using a simple 2-state model suggested that MCR was reduced at lower preload (Table 3), in contrast to the experimental data showing an increase. The fit to the shortened preload resulted in a substantially increased cooperativity and faster rates of myosin attachment and detachment (Supplemental Table 2).

Because this most simple myosin model was not consistent with experimental data, we next fit a 3-state model with two attached states to allow for a power stroke (Supplemental Figure 2B). The fit again showed limitations and did not fully replicate experimental tension traces (Fig. 3), and it again resulted in a reduced MCR at reduced preload, albeit to a smaller extent than the 2-state model (Table 3). The improvement in the MCR was coincident with an increase in the power-stroke transition by approximately 10% (Supplemental Table 3). The 3-state model did not include a reverse rate that would allow a weakly bound myosin head to detach before performing the power-stroke. This is because inclusion of such state caused a delay in the start of relaxation and a sudden loss of force that did not mimic the

Health Research Alliance Author Manuscript

Health Research Alliance Author Manuscript

experimental condition (Supplemental Figure 5). Fixing thin filament parameters from the Lo fit as constants but allowing myosin parameters to be modified resulted in a reduced MCR at shorter lengths while further accelerating the power stroke. Setting the thick filament parameters from the Lo fit did not substantially improve the MCR and resulted in substantial accelerations of the thin filament activation and deactivation rates, along with an increase in cooperativity. We also confirmed that the reduced MCR at reduced preload was not dependent on the initial half-sarcomere length of the model. Shorter predicted Lo lengths did reduce absolute MCR values, but increased the percent reduction (preload dependence) of MCR at reduced preload (Supplemental Table 4).

Because these fits did not result in increases in MCR, we manually adjusted thin filament and myosin kinetic parameters to further isolate individual contributors to MCR. Parameters of the 3-state system that had been fit to the shortened length were adjusted by up to 70% above and below their original value. For thin filament parameters, decreasing the rate that binding sites open or increasing the rate that biding sites close could increase MCR (Fig. 4). However, these changes result in a substantial increase in fixed-end isometric tension, which are not expected to occur physiologically. Reducing cooperativity would increase MCR greater than the change in fixed-end isometric tension (Fig. 4). For myosin transition parameters, reducing the power-stroke rate or increasing the detachment rate could increase MCR faster than increasing the tension at reduced preloads (Fig. 5). Reducing the power-stroke transition rate would also increase MCR, but again, this rate is expected to increase at reduced preload.

We additionally evaluated whether force-dependent myosin transitions could explain the preload-dependence of Mechanical Control of Relaxation. Force dependence meant that the rate parameter would be multiplied by the total force and by a force dependent parameter. This variable also allowed both loads to be fit simultaneously. First, we evaluated the fit of a model that included a super-relaxed state (SRX) added to a two-state model [18] (Supplemental Figure 2C). Reducing preload did increase MCR under these conditions (Table 3), but the model fit resulted in an uncontrolled loss of force followed by a force recovery (Supplemental Figure 5), which did not happen in the experimental data. Furthermore, model fits began their relaxation later than identified in experiments and suffered from faster than physiologic relaxation after stretch.

We then declared force-dependence independently in each of the myosin transitions of the 3-state model. Force-dependent attachment did not increase MCR at reduced preload. Increasing the power-stroke rate and detachment rate parameters all resulted in an increased MCR, but less than the increase found in experimental data. Force-dependence on the power-stroke also led to a slower, not faster [19], transition at lower preloads. Subsequently, we evaluated whether multiple force-dependent parameters could achieve the greater than 20% increase in MCR as expected (Fig. 6). The three of four models tested with multiple force-dependent parameters all showed a greater than 20% increase in MCR at reduced preload (Table 3).

Health Research Alliance Author Manuscript

Health Research Alliance Author Manuscript

4. Discussion

There is continued interest in the mechanisms that underlie myocardial relaxation, especially given the lack of efficacious treatment options for patients suffering from diastolic dysfunction and heart failure with preserved ejection fraction [1,2]. Our work has recently sought to evaluate how a mechanical intervention, i.e. preload reduction, acts as a modifier of the relaxation rate. Previously, we showed that Mechanical Control of Relaxation (MCR) was not dependent on afterload because a stretch was both necessary and sufficient to induce changes in relaxation rate [10]. While lengthening strains before the end of systole sounds surprising, there are clinical reports that suggest the importance of such myocardial lengthening events. As noted at least as early as C. J. Wiggers [9,29], normal healthy hearts have a lengthening strain before the aortic valve closes [29,30]. The time to peak strain is delayed in several conditions that are associated with diastolic dysfunction [31], which may explain the dysfunction.

Previously, we used computational modeling to predict that cross-bridge populations fall in concert with the force during relaxation [10]. The model indicated that the lengthening caused enhanced crossbridge detachment, as was previously speculated by others [7,8]. While our initial study indicated that MCR was present in mammalian hearts from mouse to man, it was limited in the conditions investigated.

The current study sought to investigate how a preload (muscle length) adjustment modifies MCR. We observed in this study that reduced preload increases the sensitivity of strain rate to the relaxation rate, i.e. increases MCR. We subsequently used computational modeling to address potential mechanisms underlying this relationship and further discuss clinical implications of our findings. These data may have substantial clinical relevance as preload adjustment are direct and secondary targets of numerous treatments for diastolic dysfunction. While preload reduction itself is associated with a shorter contractile period and could extend the diastolic duration, the relaxation rate itself is accelerated by stretch. Therefore, MCR itself would provide for a more efficient diastolic relaxation and filling.

4.1. Thin filament mechanisms associated with preload adjustment

In addition to altering filament overlap, reducing preload has previously been shown to induce numerous biomechanical changes to sarcomeric function. Non-linear passive stiffness of titin is a well-known length-dependent property, but thin and thick filament properties are also modified with reduced preload [12,17]. Calcium sensitivity is primarily governed by troponin’s contribution to thin filament regulation and is generally reported to be reduced at reduced preload [13-15]. The effect of preload on cooperative activation is less consistent, with the Hill Coefficient being reported to increase, decrease, or remained constant [16-19] with reduced preload. Thin filament modifications are reported to accelerate the relaxation rate at shorter muscle lengths, but the effect of reduced preload on MCR has not previously been investigated.

Our experimental data did show that relaxation rate was greater at reduced preload as expected. The initial fits using a 2-state myosin scheme predicted a reduced MCR at reduced preload, and was coincident with a slowing of the thin filament activation and deactivation

Health Research Alliance Author Manuscript

Health Research Alliance Author Manuscript

rates. The 3-state schemes produced model fits that again reduced the MCR at reduced preload, but led to less substantial alterations in the thin-filament parameters. Manually varying the thin filament parameters suggested that a slowing of the activation rate or increasing the deactivation rate at lower lengths could increase MCR, but the tensions would rise substantially. A reduction in cooperativity could also result in an MCR that increased faster than the increase in tension. These computational results do not provide clear evidence that thin filament mechanisms account for the increase in MCR at reduced preload.

4.2. Model predictions of the effect of myosin kinetics on Mechanical Control of Relaxation

Myosin kinetics are also reported to be modified when preload is reduced. Previously, Tanner et al. showed that reducing preload by 15% would nearly double the myosin ADP release rate [19]. Simply adding a myosin transition between attachment and detachment to mimic a power-stroke (3-state scheme) reduced the model-estimated difference in MCR from Lo to a shortened preload. However, the model still did not replicate the increase in MCR observed in the experimental data.

Recently, the super-relaxed (SRX) state of myosin was shown to improve the fit to fixed-end isometric twitches of rabbit trabeculae when added to a 2-state myosin model [18]. The SRX state is thought to be a force-dependent condition that sequesters myosin heads from attaching to actin at low force conditions. The sequestered heads are more likely to be primed for contraction at high forces, partially explaining the Frank-Starling Mechanism. The prior study provided excellent fit of isometric conditions [18]. Because this model could more quickly reduce the number of cycling heads (by inhibiting re-attachment and cycling through the ATPase process), we evaluated its effect. Indeed, the SRX state did lead to a slight increase in MCR at reduced preload, but at the expense of mimicking the relaxation rate properly upon re-stretch. Specifically, this model resulted in the tension suddenly dropping below the basal (diastolic) tension. This was followed by an increase in tension through diastole. Experimental samples did not display this feature. Thus, our models suggest that the SRX state might not be the key mechanism underlying the preload-dependence of MCR.

Model fitting using single force-dependent transitions suggests that myosin kinetics are responsible for the increase in MCR at reduced preload. Force-dependence of the power-stroke and myosin detachment parameters increased MCR at reduced preload. This result is not entirely surprising as some previous studies show changes in the rate of force redevelopment (k_{tr}) [32,33]. However, force-dependence of the power-stroke transition would decrease the power-stroke transition rate at shorter lengths instead of increasing it as expected [19]. Furthermore, the strain-dependent power-stroke again caused the tension to suddenly drop after stretch. Including multiple-force dependent parameters led to the preload-dependent change in MCR to come closer to mimicking the experimental data. Importantly, models including the force-dependence of the power-stroke and the strain-sensitivity of the detachment rate most closely matched the experimental change (although they continued to over-estimate the MCR values). These data suggest that the power-stroke and detachment rates are strain sensitive.

Health Research Alliance Author Manuscript

Health Research Alliance Author Manuscript

While these results provide strong evidence that myosin kinetics modifies MCR, we did not conclusively determine which transition(s) between myosin states dominates this effect. For one, model fits including both isometric and load-clamped data always fit less well than the isometric conditions alone. This is reflected in the often-delayed time to peak shortening and prolonged contractions observed in our models. We pursued model fitting with and without force-dependence of myosin transition parameters to evaluate the consistency of the models. Both methods have benefits. For example, fitting each preload independently allows us to investigate changes in all parameters, including those in the thin filament. In contrast, the modeling environment we utilized (MyoSim) allows force-dependence of myosin parameters which allows us to simultaneously fit two preloads [18]. However, the current force-dependent transitions in MyoSim were limited to increasing their value at increased force.

It is also possible that our model systems were insufficient to mimic true sarcomere kinetics, especially given that most models could not accurately fit the isometric data. While fixed calcium transient parameters could have contributed to poor fits, our study focused on sarcomeric parameters where we were, for example, unable to apply force-dependence to thin filament parameters. We did observe that multiple force-dependent transitions did better replicate the experimentally derived dependence of preload on MCR. However, we may be missing essential states of myosin cycling. One state that has been previously investigated in computational models but not included in the current study is a strain-dependent detached myosin-ADP state [24,34,35]. This post-power stroke, pre-ADP release state has been included in a MyoSim-based model resulting in excellent reproduction of k_{tr} with the inclusion of this state [24]. As this state is both part of the power-stroke and a detached state, it is possible that this state and its associated transitions could contribute to the changes observed in the 3-state model with multiple force-dependent transitions. A recent modeling study by Palmer et al. also speculated about the existence of this transiently detached state, even though it was not explicitly included in their model [36]. While there is at least one experimental report that may suggest such a transiently detached state exists in muscles undergoing a lengthening strain [37], experimental evidence is limited. While improvements to our understanding of sarcomeric kinetics and the modeling of the kinetics remain, these models and data suggest that the steps of myosin cycling are not yet fully characterized.

4.3. Muscle attachments and Mechanical Control of Relaxation

While MCR generally increases with reduced muscle length, some of our muscles showed reduced MCR with reduced preload (Fig. 2). An experimental factor that appears to influence preload-dependence of MCR is the quality of the attachment of the trabeculae to the force transducer and motor hooks. These attachments provide biophysical series-elastic links between the force-generating crossbridges and the ends of the muscle [24]. In permeabilized muscles, the myocardial fibers dissected are often free of chordae and mounted using aluminum clips or tie-downs with very little compliance. In contrast, intact muscles have several areas of increased end-compliance. An intact papillary muscle has non-contractile compliance (series elasticity) if it is hooked in the valve plane instead of the muscle. Both intact trabeculae and papillary muscles might also have a compliant link if a ‘basket’ mount is used, where an end of the muscle rests within a metal basket but

Health Research Alliance Author Manuscript

Health Research Alliance Author Manuscript

is not fixed to the transducer or motor [38]. This is because the muscle could slip as it is rapidly shortened or lengthened. In the current experiment, we did not use a basket mount. Nevertheless, upon post-hoc inspection, we identified 6 trabeculae with gaps and/or chordae attachments that may allow for slippage. Four of these 6 muscles showed reduced instead of increased MCR upon preload reduction. Notably, the only parameter that differed between the groups was the minimum (diastolic) tension, which was reduced in the group with potentially impaired attachments. We did not otherwise observe substantial compliance in the muscular segments that were observed, but they too could contribute to this compliance. The reduced tension would correlate with the changed end-compliance of a damaged or basket-mounted muscle. We speculate that slippage and/or change in the series elastic elements dominate this change.

These data may serve to be an experimental caution as non-contractile series elements do not appear to play a role in the intact heart [39]. This is physiologically reasonable, as the myocardium is densely packed and is synchronously contractile. Thus, except cases like infarction or desynchrony, the myocardium will typically not interact with unusual elastic elements. Physiological differences can occur in intact muscles with non-physiologic compliances. For example, Parmley et al. showed that force-calcium curves attenuated when compliance increased [40]. While we observe no substantial change in isometric behavior based on these compliant regions, when physiologic (or substantial internal) shortening does occur, it is likely to alter myocardial forces. Thus, caution may be warranted when translating experiments that utilize the basket attachment or papillary muscles when physiologic strains are induced [9,10].

4.4. Potential clinical relevance of Mechanical Control of Relaxation

This finding may have important biophysical consequences but may also be of value in interpreting clinical studies. Afterload, not preload, is a commonly studied mechanical mechanism to modify the relaxation rate [7]. Indeed, several studies using intact hearts and in vivo methods have correlated reduced afterload with improved relaxation. Our initial study of MCR showed that the lengthening strain was not only necessary but was also sufficient to modify the relaxation rate at any afterload [10]. Our prior study also showed that reduced afterload would increase the potential magnitude of the lengthening strain, again allowing for a substantially increased relaxation rate.

While there has not yet been a clear test of MCR in vivo, several possible mechanisms exist to suggest that our findings are relevant in vivo. For example, the use of diuretics to reduce afterload also modifies ventricular preload. There is also direct evidence for preload-dependent cardiac torsion [41], which supports our hypothesis that MCR is active in the in vivo context. Myocardial strain and strain rate have not traditionally been monitored in studies investigating relaxation. However, a study in the open chest dog found that systolic length was directly correlated with the relaxation rate [42]. These data indicate the importance of examining the strain rate as the mechanical modifier of the relaxation rate. The accelerated relaxation may be related to the preload-dependence of MCR as improved diastolic function appears to be coincident with a reduction in left ventricular volume in vivo.

Health Research Alliance Author Manuscript

Health Research Alliance Author Manuscript

4.5. Limitations of experimental and computational data

The primary limitation of our cardiac modeling is that some data could not be calculated or validated specifically. For example, our model utilized the calcium transient shape derived from a trabeculae loaded with Fura-2AM., which suggested the calcium transient was relatively constant at different loads and changes in strain. However, the traces did show substantial noise, which may lead to over- or under-estimation of the calcium concentration at any timepoint. We and others [27] did not observe a preload-dependence in the calcium transients with our data, and conflicting data have been reported in previous studies [13,18]. The time course and magnitude of our calcium transient was also the same for both fixed-end isometric and load-clamp twitches at the same preload. While some studies have reported changes in the calcium concentration following a load-clamp [25,27] and due to shortening alone [43], we chose to use the same one based on our data because each study used different conditions. This allowed for more model parsimony, allowing us to focus on the sarcomeric properties underlying the preload-dependence of MCR while minimizing overfitting with extraneous calcium transient parameters. It is also possible that a slow binding rate of our fluorophore might have led us to predict that the calcium transient did not decay fast enough. This could contribute to the inability of our models to relax as early as the experimental data. Methodological refinements or the use of alternate fluorophores, or the recently reported thin-filament biosensor [44], may provide added precision and accuracy for future models.

Furthermore, we experimentally utilized muscle length, which had to be translated to sarcomere and series elastic element lengths in the model. We were not able to directly measure sarcomere length in this study; therefore, we were not able to validate the specific shortening and relenthening of the simulated twitches. However, preliminary studies on fixed tissues indicate a range of sarcomere lengths at Lo from 2.15 to 2.4 μm (data not shown), within the range of previously reported lengths [13,22,38]. Importantly, muscle-level properties are more appropriate for translational application as the sarcomeric lengths (and inhomogeneities) are not represented in clinical strain and strain rate imaging [7,10,24,45]. Experimentally, both the shortening magnitude and strain rate increased at lower preloads. Our computational model also often failed to replicate the changes in shortening and strain rate achieved experimentally, severely underestimating the change in shortening and predicting a reduced strain at reduced preloads. It is unclear why this is the case, but the estimated series elasticity may not have accurately represented the physiology. Detailed imaging study may be required to evaluate how the series elements or sarcomeres in series might modify this response. Further experimental and modeling studies focusing on the series elastic components may be warranted.

5. Conclusions

Impaired myocardial relaxation is an early indicator of diastolic dysfunction. While the biochemical kinetic properties of calcium transients, thin filament activation, and the myosin ATPase can modify relaxation, the relaxation rate is also mechanically modified by lengthening strain rates. This is termed Mechanical Control of Relaxation. The experimental data shows that MCR can be enhanced by reducing preload. This mechanism may provide

Health Research Alliance Author Manuscript

Health Research Alliance Author Manuscript

additional insight into in vivo clinical work where treatments for diastolic dysfunction remain limited but where volume reduction can improve relaxation. Our computational modeling studies provide further insight into molecular mechanisms, suggesting myosin's kinetic and strain dependent properties underlie the preload-dependence of MCR. The results also indicate that simple models of myosin kinetics still do not provide perfect models of muscle twitches and length changes. Nonetheless, this mixture of biophysical experimentation and computational modeling of muscles provides new insights into preload-dependent modifiers of myocardial relaxation.

Supplementary Material

Refer to Web version on PubMed Central for supplementary material.

Acknowledgements

Supported by the American Heart Association (14SDG20100063 and 18TPA34170169) to CSC. Additional support provided by the School of Medicine Summer Undergraduate Research Experience (BMS, TLC) and Integrative Biomedical Sciences Programs (MJB), Department of Physiology Summer Undergraduate Research Fellowship (TLC), and the Richard Barber Interdisciplinary Research Program (HD) at Wayne State University.

Abbreviations:

MCR	Mechanical Control of Relaxation, or the relationship between the end systolic strain rate and relaxation rate
Lo	Muscle length providing optimal/maximal developed force
CSA	Cross-sectional area
SRX	Super-relaxed state of myosin

References

[1]. Pieske B, Tschope C, de Boer RA, Fraser AG, Anker SD, Donal E, Edelmann F, Fu M, Guazzi M, Lam CSP, Lancellotti P, Melenovsky V, Morris DA, Nagel E, Pieske-Kraigher E, Ponikowski P, Solomon SD, Vasan RS, Rutten FH, Voors AA, Ruschitzka F, Paulus WJ, Seferovic P, Filippatos G, How to diagnose heart failure with preserved ejection fraction: the HFA-PEFF diagnostic algorithm: a consensus recommendation from the Heart Failure Association (HFA) of the European Society of Cardiology (ESC), Eur. Heart J 40 (40) (2019) 3297–3317. [PubMed: 31504452]

[2]. Shah SJ, Borlaug BA, Kitzman DW, McCulloch AD, Blaxall BC, Agarwal R, Chirinos JA, Collins S, Deo RC, Gladwin MT, Granzier H, Hummel SL, Kass DA, Redfield MM, Sam F, Wang TJ, Desvigne-Nickens P, Adhikari BB, Research priorities for heart failure with preserved ejection fraction: national heart, lung, and blood institute working group summary, Circulation 141 (12) (2020) 1001–1026. [PubMed: 32202936]

[3]. Biesiadecki BJ, Davis JP, Ziolo MT, Janssen PM, Tri-modal regulation of cardiac muscle relaxation; intracellular calcium decline, thin filament deactivation, and cross-bridge cycling kinetics, Biophys Rev 6 (3-) (2014) 273–289. [PubMed: 28510030]

[4]. Janssen PM, Kinetics of cardiac muscle contraction and relaxation are linked and determined by properties of the cardiac sarcomere, American journal of physiology, Heart and circulatory physiology 299 (4) (2010) H1092–H1099. [PubMed: 20656885]

Health Research Alliance Author Manuscript

Health Research Alliance Author Manuscript

[5]. Chung JH, Canan BD, Whitson BA, Kilic A, Janssen PML, Force-frequency relationship and early relaxation kinetics are preserved upon sarcoplasmic blockade in human myocardium, Phys. Rep 6 (20) (2018), e13898.

[6]. Mannozzi J, Massoud L, Kaur J, Coutsos M, O'Leary DS, Ventricular contraction and relaxation rates during muscle metaboreflex activation in heart failure: are they coupled? Exp. Physiol 106 (2) (2021) 401–411, 10.1113/EP089053. Epub 2020 Dec 9. PMID: 33226720 PMCID: PMC7855894. [PubMed: 33226720]

[7]. Brutsaert DL, Rademakers FE, Sys SU, Triple control of relaxation: implications in cardiac disease, Circulation 69 (1) (1984) 190–196. [PubMed: 6227428]

[8]. Brutsaert DL, Housmans PR, Goethals MA, Dual control of relaxation. Its role in the ventricular function in the mammalian heart, Circ. Res 47 (5) (1980) 637–652. [PubMed: 6106532]

[9]. Chung CS, How myofilament strain and strain rate lead the dance of the cardiac cycle, Arch. Biochem. Biophys 664 (2019) 62–67. [PubMed: 30710504]

[10]. Chung CS, Hoopes CW, Campbell KS, Myocardial relaxation is accelerated by fast stretch, not reduced afterload, J. Mol. Cell. Cardiol 103 (2017) 65–73. [PubMed: 28087265]

[11]. Streeter DD Jr., Hanna WT, Engineering mechanics for successive states in canine left ventricular myocardium. II. Fiber angle and sarcomere length, Circ. Res 33 (6) (1973) 656–664. [PubMed: 4762007]

[12]. Chung CS, Granzier HL, Contribution of titin and extracellular matrix to passive pressure and measurement of sarcomere length in the mouse left ventricle, J. Mol. Cell. Cardiol 50 (4) (2011) 731–739. [PubMed: 21255582]

[13]. Allen DG, Kentish JC, The cellular basis of the length-tension relation in cardiac muscle, J. Mol. Cell. Cardiol 17 (9) (1985) 821–840. [PubMed: 3900426]

[14]. Dupuis LJ, Lumens J, Arts T, Delhaas T, High tension in sarcomeres hinders myocardial relaxation: a computational study, PloS One 13 (10) (2018), e0204642. [PubMed: 30286135]

[15]. Hanft LM, Biesiadecki BJ, McDonald KS, Length dependence of striated muscle force generation is controlled by phosphorylation of cTnI at serines 23/24, J. Physiol 591 (18) (2013) 4535–4547. [PubMed: 23836688]

[16]. Monasky MM, Biesiadecki BJ, Janssen PM, Increased phosphorylation of tropomyosin, troponin I, and myosin light chain-2 after stretch in rabbit ventricular myocardium under physiological conditions, J. Mol. Cell. Cardiol 48 (5) (2010) 1023–1028. [PubMed: 20298699]

[17]. Lee EJ, Nedrud J, Schemmel P, Gotthardt M, Irving TC, Granzier HL, Calcium sensitivity and myofilament lattice structure in titin N2B KO mice, Arch. Biochem. Biophys 535 (1) (2013) 76–83. [PubMed: 23246787]

[18]. Campbell KS, Janssen PML, Campbell SG, Force-Dependent Recruitment from the Myosin off State Contributes to Length-dependent Activation, Biophys J, 2018.

[19]. Tanner BC, Breithaupt JJ, Awinda PO, Myosin MgADP release rate decreases at longer sarcomere length to prolong myosin attachment time in skinned rat myocardium, Am. J. Physiol. Heart Circ. Physiol 309 (12) (2015) H2087–H2097. [PubMed: 26475586]

[20]. Campbell KS, Moss RL, SLControl: PC-based data acquisition and analysis for muscle mechanics, Am. J. Physiol. Heart Circ. Physiol 285 (6) (2003) H2857–H2864. [PubMed: 12907419]

[21]. Schotola H, Sossalla ST, Renner A, Gummert J, Danner BC, Schott P, Toischer K, The contractile adaption to preload depends on the amount of afterload, ESC heart failure 4 (4) (2017) 468–478. [PubMed: 29154423]

[22]. Ait-Mou Y, Zhang M, Martin JL, Greaser ML, de Tombe PP, Impact of titin strain on the cardiac slow force response, Prog. Biophys. Mol. Biol (2017).

[23]. Raff GL, Glantz SA, Volume loading slows left ventricular isovolumic relaxation rate. Evidence of load-dependent relaxation in the intact dog heart, Circ. Res 48 (6 Pt 1) (1981) 813–824. [PubMed: 7226443]

[24]. Campbell KS, Dynamic coupling of regulated binding sites and cycling myosin heads in striated muscle, J. Gen. Physiol 143 (3) (2014) 387–399. [PubMed: 24516189]

Health Research Alliance Author Manuscript

Health Research Alliance Author Manuscript

[25]. Rice JJ, Wang F, Bers DM, de Tombe PP, Approximate model of cooperative activation and crossbridge cycling in cardiac muscle using ordinary differential equations, Biophys. J 95 (5) (2008) 2368–2390. [PubMed: 18234826]

[26]. Stuyvers BD, Miura M, ter Keurs HE, Dynamics of viscoelastic properties of rat cardiac sarcomeres during the diastolic interval: involvement of Ca2+, J. Physiol 502 (Pt 3) (1997) 661–677. [PubMed: 9279816]

[27]. Backx PH, Ter Keurs HE, Fluorescent properties of rat cardiac trabeculae microinjected with fura-2 salt, Am. J. Physiol 264 (4 Pt 2) (1993) H1098–H1110. [PubMed: 8476086]

[28]. Janssen PM, Stull LB, Marban E, Myofilament properties comprise the rate-limiting step for cardiac relaxation at body temperature in the rat, Am. J. Physiol. Heart and circulatory physiology 282 (2) (2002) H499–H507.

[29]. Wiggers CJ, Studies on the consecutive phases of the cardiac cycle I. The duration of the consecutive phases of the cardiac cycle and the criteria for their precise determination, Am. J. Physiol 56 (3) (1921) 415–438.

[30]. Rosen BD, Gerber BL, Edvardsen T, Castillo E, Amado LC, Nasir K, Kraitchman DL, Osman NF, Bluemke DA, Lima JA, Late systolic onset of regional LV relaxation demonstrated in three-dimensional space by MRI tissue tagging, Am. J. Physiol. Heart Circ. Physiol 287 (4) (2004) H1740–H1746. [PubMed: 15205167]

[31]. Saito M, Okayama H, Yoshii T, Hiasa G, Sumimoto T, Inaba S, Nishimura K, Inoue K, Ogimoto A, Ohtsuka T, Funada J, Shigematsu Y, Higaki J, The differences in left ventricular torsional behavior between patients with hypertrophic cardiomyopathy and hypertensive heart disease, Int. J. Cardiol 150 (3) (2011) 301–306. [PubMed: 20471702]

[32]. Adhikari BB, Regnier M, Rivera AJ, Kreutziger KL, Martyn DA, Cardiac length dependence of force and force redevelopment kinetics with altered cross-bridge cycling, Biophys. J 87 (3) (2004) 1784–1794. [PubMed: 15345557]

[33]. Milani-Nejad N, Xu Y, Davis JP, Campbell KS, Janssen PM, Effect of muscle length on cross-bridge kinetics in intact cardiac trabeculae at body temperature, J. Gen. Physiol 141 (1) (2013) 133–139. [PubMed: 23277479]

[34]. Smith DA, Geeves MA, Strain-dependent cross-bridge cycle for muscle. II. Steady-state behavior, Biophys. J 69 (2) (1995) 538–552. [PubMed: 8527668]

[35]. Chung CS, Move quickly to detach: strain rate-dependent myosin detachment and cardiac relaxation, J. Gen. Physiol 152 (4) (2020).

[36]. Palmer BM, Swank DM, Miller MS, Tanner BCW, Meyer M, LeWinter MM, Enhancing diastolic function by strain-dependent detachment of cardiac myosin crossbridges, J. Gen. Physiol 152 (4) (2020).

[37]. Amemiya Y, Iwamoto H, Kobayashi T, Sugi H, Tanaka H, Wakabayashi K, Time-resolved X-ray diffraction studies on the effect of slow length changes on tetanized frog skeletal muscle, J. Physiol 407 (1988) 231–241. [PubMed: 3267188]

[38]. de Tombe PP, ter Keurs HE, Force and velocity of sarcomere shortening in trabeculae from rat heart, Effects of temperature, Circ Res 66 (5) (1990) 1239–1254. [PubMed: 2335024]

[39]. Campbell KB, Kirkpatrick RD, Tobias AH, Taheri H, Shroff SG, Series coupled non-contractile elements are functionally unimportant in the isolated heart, Cardiovasc. Res 28 (2) (1994) 242–251. [PubMed: 8143307]

[40]. Parmley WW, Chuck L, Clark S, Matthews A, Effects of added compliance on force-velocity relations calculated from isometric tension records, Am. J. Physiol 225 (6) (1973) 1271–1275. [PubMed: 4760439]

[41]. Burns AT, La Gerche A, D'Hooge J, MacIsaac AI, Prior DL, Left ventricular strain and strain rate: characterization of the effect of load in human subjects, Eur. J. Echocardiogr 11 (3) (2010) 283–289. [PubMed: 20026455]

[42]. Gaasch WH, Blaustein AS, Adam D, Myocardial relaxation IV: mechanical determinants of the time course of left ventricular pressure decline during isovolumic relaxation, Eur. Heart J Suppl. (1980) 111–117.

Health Research Alliance Author Manuscript

Health Research Alliance Author Manuscript

[43]. Housmans PR, Lee NK, Blinks JR, Active shortening retards the decline of the intracellular calcium transient in mammalian heart muscle, Science 221 (4606) (1983) 159–161. [PubMed: 6857274]

[44]. Vetter AD, Martin AA, Thompson BR, Thomas DD, Metzger JM, Sarcomere integrated biosensor detects myofilament-activating ligands in real time during twitch contractions in live cardiac muscle, J. Mol. Cell. Cardiol 147 (2020) 49–61. [PubMed: 32791214]

[45]. Campbell SG, Hatfield PC, Campbell KS, A mathematical model of muscle containing heterogeneous half-sarcomeres exhibits residual force enhancement, PLoS Comput. Biol 7 (9) (2011), e1002156. [PubMed: 21980268]

Health Research Alliance Author Manuscript

Health Research Alliance Author Manuscript

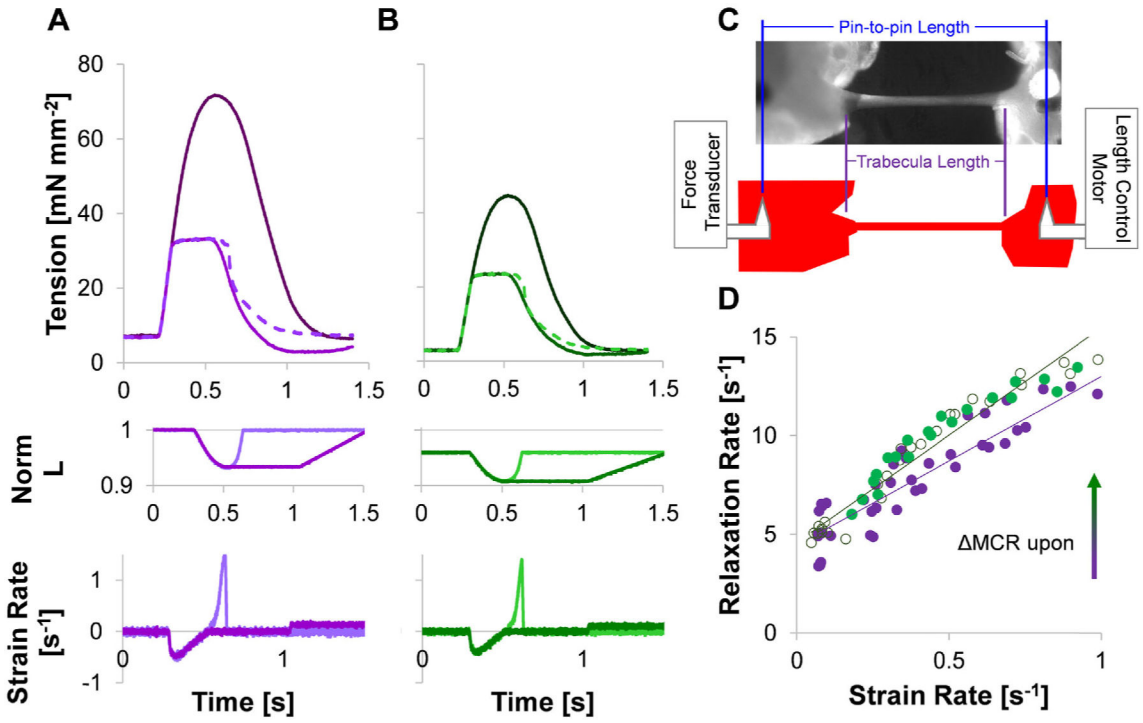

Fig. 1.

Example experimental data. A&B) Tension, Length normalized to Lo, and strain rate for a muscle at Lo (Panel A, purple) and a muscle reduced in length (Panel B, green) to 0.96 Lo of the trabeculae length (0.975 Lo of pin-to-pin length). An isometric trace (dark solid), a load-clamp with no relengthening (solid line), and a load-clamp trace fully relengthened (dashed line) are shown. C) Image of the cardiac trabeculae at Lo and schematic of mounting. Trabeculae length was used unless otherwise stated. D) Mechanical Control of Relaxation (relaxation rate versus strain rate relationship) increases with reduced preload. Data from preloads shown in Panels A (purple) and B (green) are shown in solid circles; data at further reduced preload (0.92 Lo of the trabeculae length, 0.95 Lo of the muscle length) shown as open circles. See Supplementary Fig. 1 for an example of how Panel C was derived; linearity of MCR (slope) is shown in Supplementary Fig. 4.

Health Research Alliance Author Manuscript

Health Research Alliance Author Manuscript

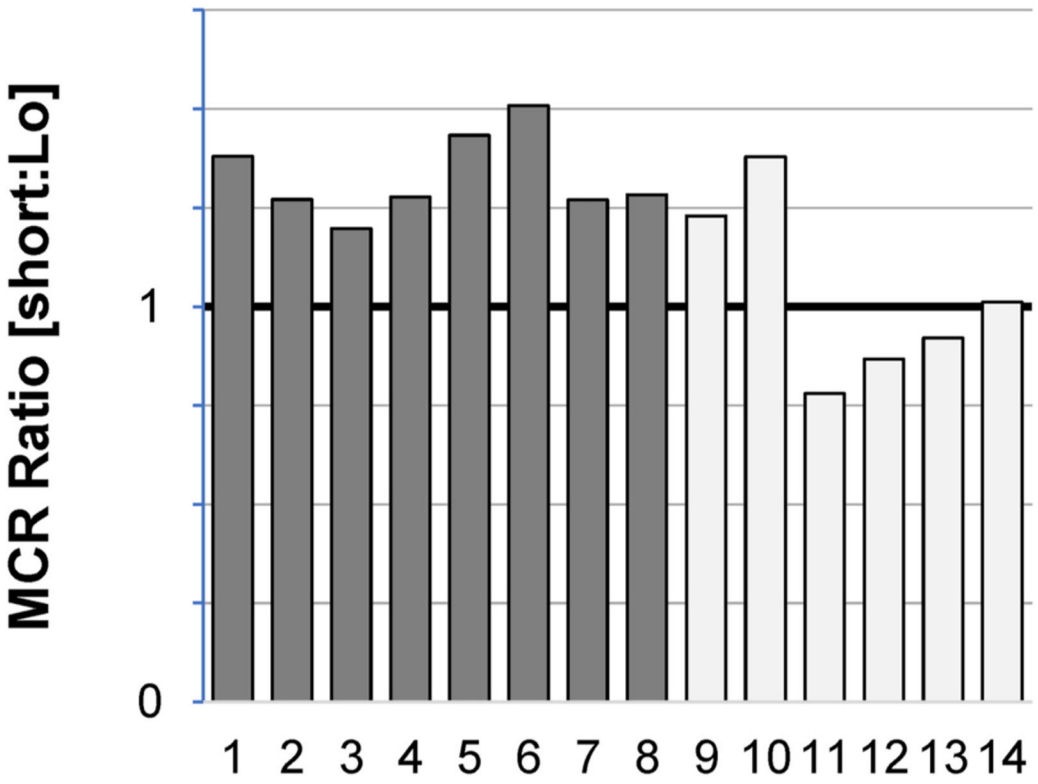

Fig. 2.

Relative MCR ratio for each trabecula. MCR was calculated for each muscle at Lo and again at reduced preload (0.95 Lo of the muscle length). Light colored shading indicates trabeculae with possible compliant attachments. On average, MCR increased by 20% ($p < 0.001$, one sample *t*-test, n = 14).

Health Research Alliance Author Manuscript

Health Research Alliance Author Manuscript

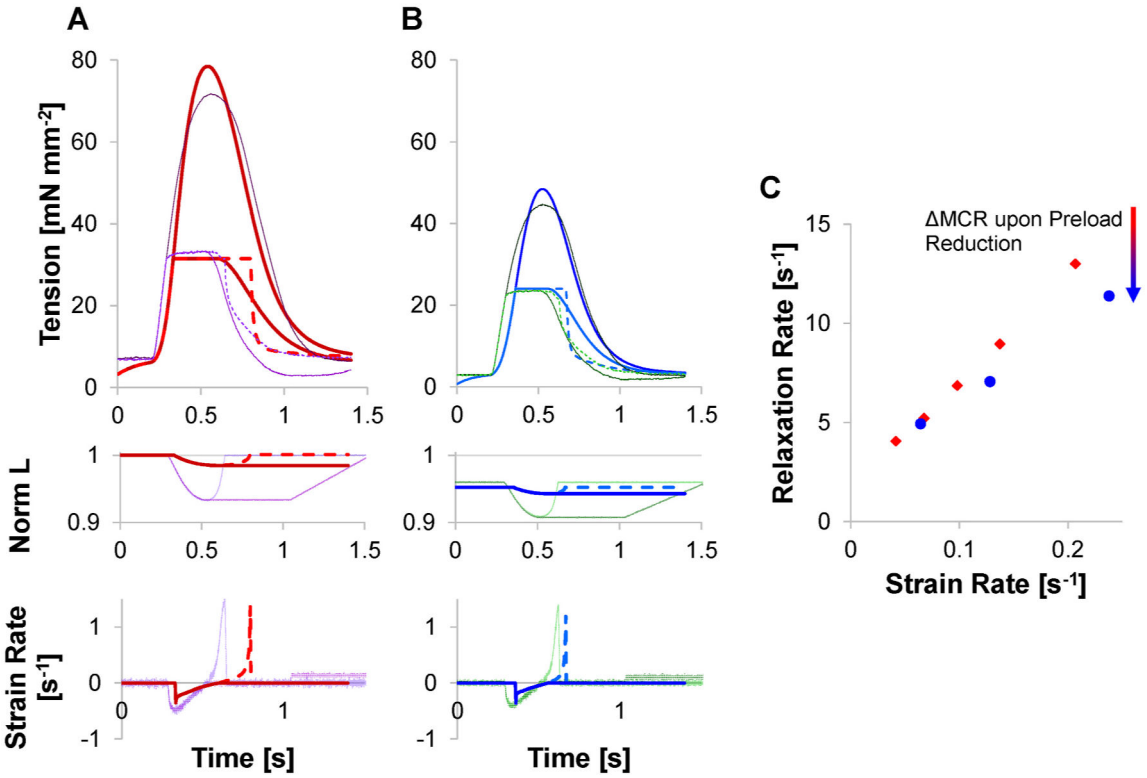

Fig. 3.

Model predicted forces of the 2-state myosin model based on fits to experimental data for the muscle at Lo (A, red lines) and reduced preload (B, blue lines). Length was calculated relative to trabecula length at Lo. Experimental data (Fig. 1) shown as thin lines (purple and green, respectively). The computed MCR data (C) for this model shows slopes greater than the experiment and do not replicate the preload dependent increase in MCR.

Health Research Alliance Author Manuscript

Health Research Alliance Author Manuscript

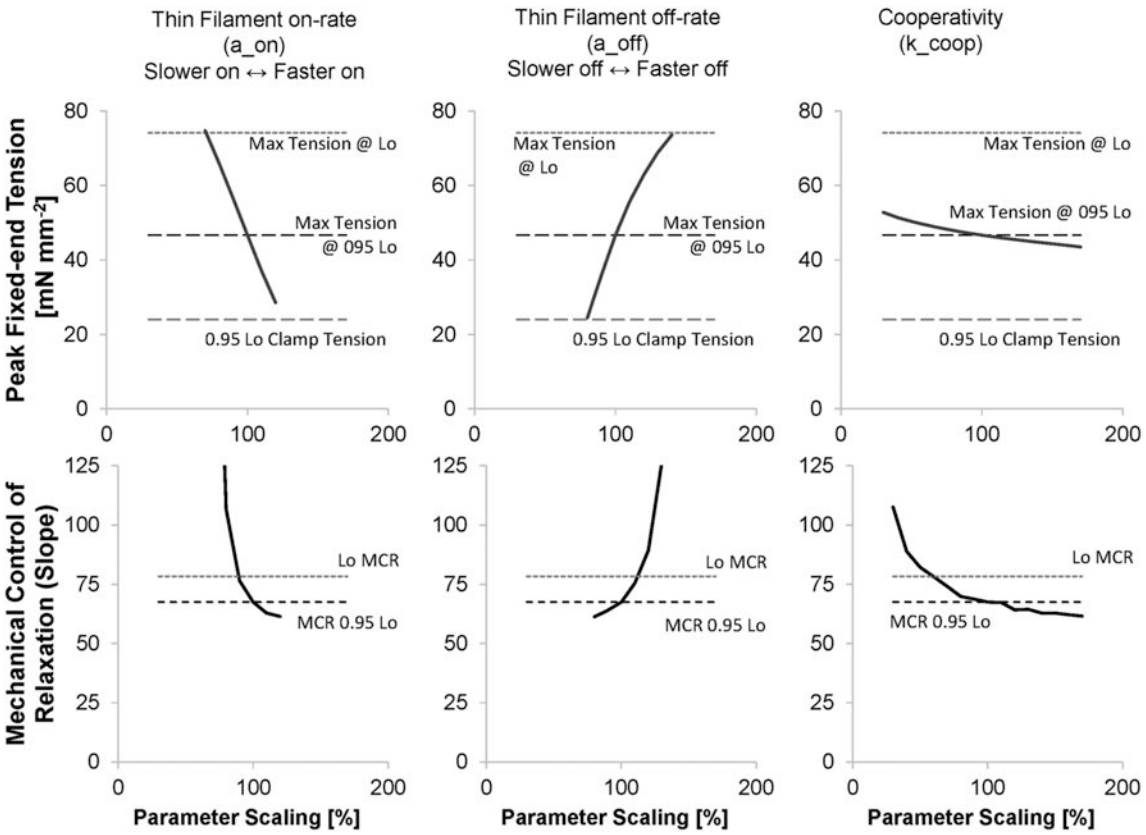

Fig. 4.

Peak fixed-end isometric tension and MCR after manual scaling of thin filament parameters. Parameter variation based on the 3-state mode with no force-dependent transitions. Only reduced cooperativity increases MCR faster than peak tension.

Health Research Alliance Author Manuscript

Health Research Alliance Author Manuscript

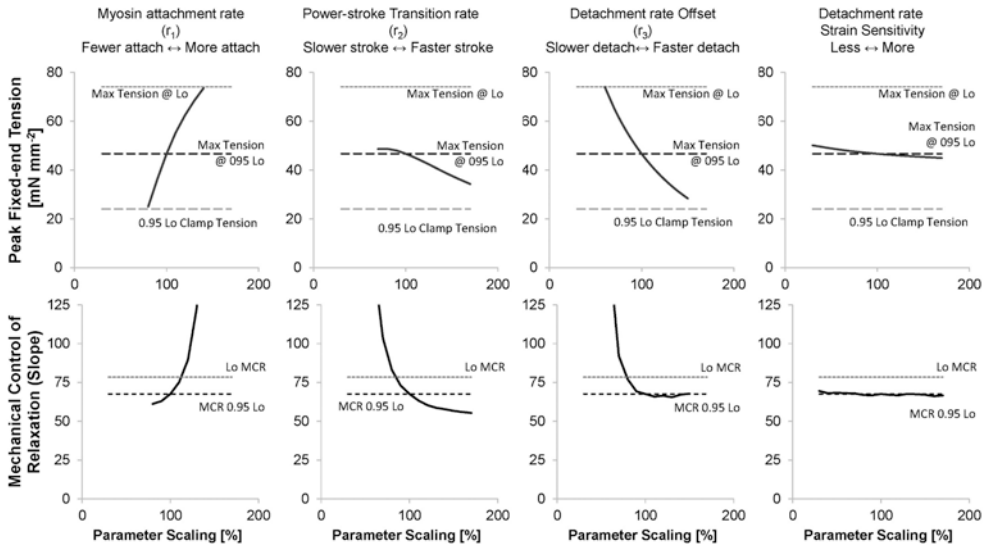

Fig. 5.

Peak fixed-end isometric tension and Mechanical Control of Relaxation after manual scaling of myosin transition rate parameters. Parameter variation based on the 3-state mode with no force-dependent transitions.

Health Research Alliance Author Manuscript

Health Research Alliance Author Manuscript

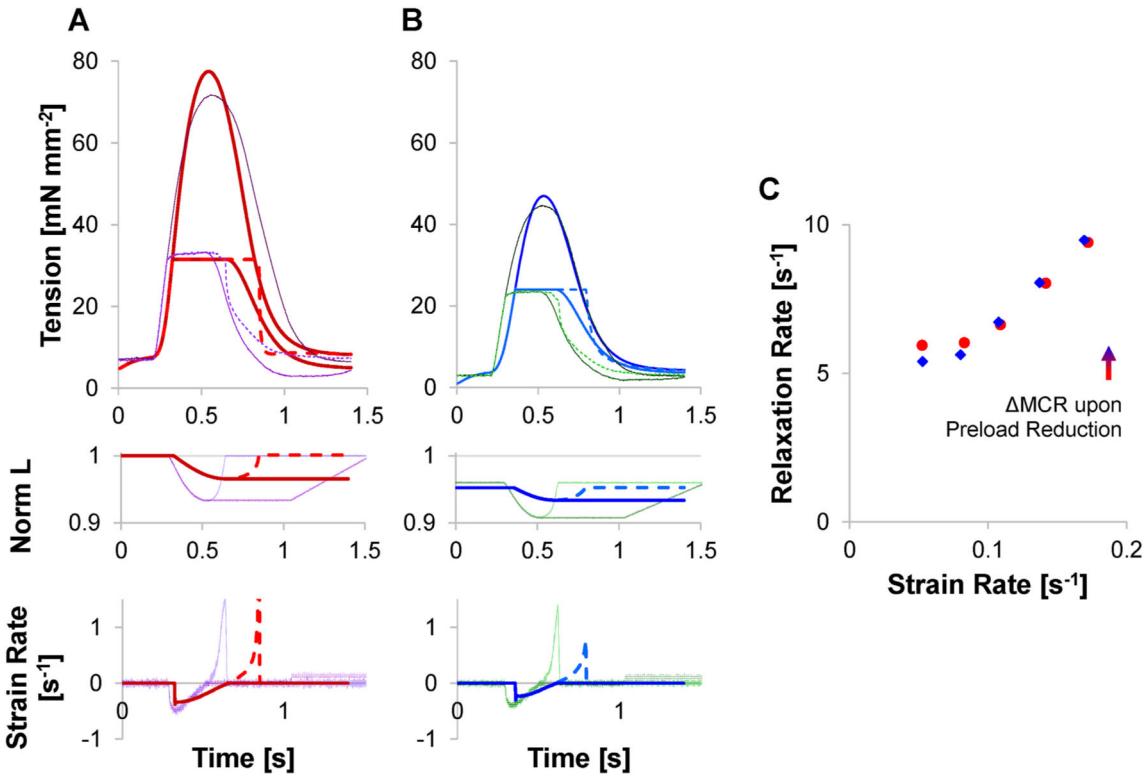

Fig. 6.

Model predicted forces of a 3-state model with force dependent detachment rates based on fits to experimental data for the muscle at Lo (A, redlines) and reduced preload (B, blue lines). Experimental data (Fig. 1) shown as thin lines (purple and green, respectively). Model fits continue to result in delayed and/or slowed isometric relaxation and a non-physiologic, accelerated relaxation after stretch. However, the computed MCR data (C) for this model begin to replicate the preload dependence observed in the experimental data.

Health Research Alliance Author Manuscript

Health Research Alliance Author Manuscript

Table 1

Rat body and trabeculae parameters for the 14 samples analyzed in this study. Developed Tensions reported for fixed-end twitches. P-values listed are based on paired *t*-test of values from 0.95 Lo versus Lo conditions.

Rat Body Parameters	**Mean ± SD**	**Range [Min, Max]**
Age [months]	4.3 ± 1.1	[3.1, 6.0]
Body Weight [g]	224 ± 29	[172, 273]
Trabeculae Parameters	**Mean ± SD**	**Range [Min, Max]**
Length at optimal force development (Lo) [mm]	2.25 ± 0.43	[1.66, 2.88]
Cross-sectional area (CSA) [mm^2]	0.074 ± 0.082	[0.012, 0.332]
Minimum (Diastolic) Tension at Lo [mN/mm^2]	3.3 ± 2.0	[0.9 ± 6.7]
Developed Tension at Lo [mN/mm^2]	37.9 ± 16.7	[10.3, 72.2]
Developed Tension at 0.95 Lo [mN/mm^2]	20.9 ± 8.9 $p < 0.001$	[6.7, 40.0]
Fixed-end relaxation rate at Lo [s^{-1}]	8.9 ± 4.4	[3.1, 20.7]
Fixed-end relaxation rate at 0.95 Lo [s^{-1}]	10.7 ± 3.4 $p = 0.009$	[3.7, 17.2]

Health Research Alliance Author Manuscript

Health Research Alliance Author Manuscript

Table 2

Experimental MCR values. Six samples had impaired attachment points by inspection, which affected the change in slope. P-values listed are based on paired *t*-test of values from 0.95 Lo versus Lo conditions.

	N	MCR at Lo	MCR at Reduced Preload (0.95 Lo)	Percent Change in MCR	p-value (Paired T-test)
All Trabeculae	14	12.7± 3.8	15.2 ± 5.0	21 ± 23	$p < 0.001$
Trabeculae without impaired attachment points	8	12.5 ± 4.4	16.6 ± 5.7	34 ± 12	$p < 0.001$
Trabeculae with impaired attachment points	6	13.1 ± 3.5	13.3 ± 3.5	3 ± 23	$p = 0.097$

Health Research Alliance Author Manuscript

Health Research Alliance Author Manuscript

Table 3

Mechanical Control of Relaxation (MCR) predictions for model fits. For models without force-dependence, each preload was fit independently. Fixed parameters refer to parameters unchanged from the fit used to derive the MCR at Lo. For data with force-dependent states, both preloads were fit simultaneously with only one force-dependent parameter. Model-simulated tensions, normalized length, and strain-rates shown in Supplemental Figure 5.

Model	MCR at Lo	MCR at Reduced Preload (0.95 Lo)	Percent Change in MCR
Models without force-dependent parameters			
2-State	54.4	37.3	−31%
3-State	78.3	71.6	−9%
3-State, fixed Thin Filament Parameters	“	54.5	−30%
3-State, fixed Thick Filament Parameters	“	72.1	−8%
Models with force-dependent parameters			
2-State with additional Force dependent SRX	42.0	46.7	+11%
3-State, Force-dependent Attachment	69.0	67.6	−2%
3-State, Force-dependent Power-stroke	44.5	49.2	+10%
3-State, Force-dependent Detachment Magnitude	45.5	48.3	+6%
3-State, Force-dependent Detachment Strain Sensitivity	46.1	50.8	+10%
Models with multiple force-dependent parameters			
3-State, Force-dependent Detachment Parameters	35.3	43.1	+22%
3-State, Force-dependent Power-stroke and Detachment Parameters	23.5	32.3	+38%
3-State, Force-dependent Power-stroke and Strain-sensitive Detachment Parameters	42.4	47.1	+11%
Force-dependent SRX and 3-State Force-dependent Power-stroke and Detachment Parameters	35.2	42.6	+21%